

Crystal Structures of Two Transcriptional Regulators from *Bacillus cereus* Define the Conserved Structural Features of a PadR Subfamily

Guntur Fibriansah^{1‡a}, Ákos T. Kovács^{2‡b}, Trijntje J. Pool¹, Mirjam Boonstra², Oscar P. Kuipers², Andy-Mark W. H. Thunnissen^{1*}

1 Laboratory of Biophysical Chemistry, Groningen Biomolecular Sciences and Biotechnology Institute, University of Groningen, Groningen, The Netherlands, **2** Department of Genetics, Groningen Biomolecular Sciences and Biotechnology Institute, University of Groningen, Groningen, The Netherlands

Abstract

PadR-like transcriptional regulators form a structurally-related family of proteins that control the expression of genes associated with detoxification, virulence and multi-drug resistance in bacteria. Only a few members of this family have been studied by genetic, biochemical and biophysical methods, and their structure/function relationships are still largely undefined. Here, we report the crystal structures of two PadR-like proteins from *Bacillus cereus*, which we named *bcPadR1* and *bcPadR2* (products of gene loci BC4206 and BCE3449 in strains ATCC 14579 and ATCC 10987, respectively). BC4206, together with its neighboring gene BC4207, was previously shown to become significantly upregulated in presence of the bacteriocin A5-48. DNA mobility shift assays reveal that *bcPadR1* binds to a 250 bp intergenic region containing the putative BC4206–BC4207 promoter sequence, while *in-situ* expression of *bcPadR1* decreases bacteriocin tolerance, together suggesting a role for *bcPadR1* as repressor of BC4206–BC4207 transcription. The function of *bcPadR2* (48% identical in sequence to *bcPadR1*) is unknown, but the location of its gene just upstream from genes encoding a putative antibiotic ABC efflux pump, suggests a role in regulating antibiotic resistance. The *bcPadR* proteins are structurally similar to LmrR, a PadR-like transcription regulator in *Lactococcus lactis* that controls expression of a multidrug ABC transporter via a mechanism of multidrug binding and induction. Together these proteins define a subfamily of conserved, relatively small PadR proteins characterized by a single C-terminal helix for dimerization. Unlike LmrR, *bcPadR1* and *bcPadR2* lack a central pore for ligand binding, making it unclear whether the transcriptional regulatory roles of *bcPadR1* and *bcPadR2* involve direct ligand recognition and induction.

Citation: Fibriansah G, Kovács ÁT, Pool TJ, Boonstra M, Kuipers OP, et al. (2012) Crystal Structures of Two Transcriptional Regulators from *Bacillus cereus* Define the Conserved Structural Features of a PadR Subfamily. PLoS ONE 7(11): e48015. doi:10.1371/journal.pone.0048015

Editor: Eric Cascales, Centre National de la Recherche Scientifique, Aix-Marseille Université, France

Received: June 27, 2012; **Accepted:** September 20, 2012; **Published:** November 26, 2012

Copyright: © 2012 Fibriansah et al. This is an open-access article distributed under the terms of the Creative Commons Attribution License, which permits unrestricted use, distribution, and reproduction in any medium, provided the original author and source are credited.

Funding: Funding was provided by the University of Groningen. Work was supported in part by an Ubbo Emmius Bursary (University of Groningen) awarded to GF. The funders had no role in study design, data collection and analysis, decision to publish, or preparation of the manuscript.

Competing Interests: The authors have declared that no competing interests exist.

* E-mail: a.m.w.h.thunnissen@rug.nl

‡a Current address: Laboratory of Virus Structure and Function, Duke-NUS Graduate Medical School, Singapore, Singapore

‡b Current address: Terrestrial Biofilms, Institute of Microbiology, Friedrich Schiller University of Jena, Jena, Germany

Introduction

Members of the PadR-like protein family (accession no. Pfam PF03551) form a large and widespread group of bacterial transcription factors that regulate diverse processes including multi-drug resistance, virulence and detoxification. They are named after the phenolic acid decarboxylation repressor, which is a transcription factor that represses genes associated with the phenolic acid stress response in gram-positive bacteria such as *Bacillus subtilis*, *Pediococcus pentosaceus*, and *Lactobacillus plantarum* [1,2]. Besides the founding member, only a few of the PadR-like proteins have been or are currently under investigation. These include AphA, which activates virulence gene expression in *Vibrio cholerae* [3], LmrR and LadR, which are repressors of genes encoding a multi-drug resistance pump in *Lactococcus lactis* and *Listeria monocytogenes*, respectively [4,5], and Pex, a regulator of circadian rhythms in *Synechococcus elongates* [6]. Crystal structures have been reported of AphA, LmrR and Pex, confirming that

these proteins share a common fold consisting of two domains: a highly conserved N-terminal winged helix-turn-helix (wHTH) domain of approximately 80–90 amino acid residues, involved in DNA-binding, and a variable C-terminal domain of one or more α -helices, involved in dimerization [7–9]. PadR-like proteins are related to members of the multiple antibiotic resistance regulator (MarR) protein family, which have similar wHTH DNA-binding domains but significantly larger and distinct C-terminal dimerization domains [10]. The size of the C-terminal domain is also a major discriminator among different PadR-like proteins, which have been classified into two distinct subfamilies [4]. PadR-like proteins of subfamily 1 (hereafter abbreviated as PadR-s1, approximately 180 amino acids), which include AphA, PadR and LadR, have relatively large C-terminal domains of about 80–90 amino acids containing multiple α -helices, while subfamily 2 PadR-like proteins (PadR-s2, approximately 110 amino acids), which includes LmrR, have significantly smaller C-terminal domains of about 20–30 amino acids forming a single α -helix.

Currently, the Protein Data Bank contains structures of only a few PadR-s2 proteins. Among these proteins, LmrR is the only one that has been studied both structurally and functionally: the structures of the other proteins were solved by structural genomics centers without a published record of their functional properties. LmrR regulates the expression of LmrCD, a major multidrug ABC efflux pump of *L. lactis* [11], via a mechanism involving multidrug binding and induction [5,9]. Forming a negative feedback loop, LmrR also regulates transcription of its own gene, which is situated just upstream from the *lmrCD* genes, [12]. Crystal structures of LmrR in complex with different ligands revealed that LmrR contains an unusual multidrug binding site within a large central hydrophobic pore at its dimer interface [9]. Multidrug recognition is dominated by aromatic stacking interactions of the flat heterocyclic cores of the ligands with opposing indole groups of two dimer-related tryptophan residues (W96/W96'), the prime indicating the dimer-related subunit). Interestingly, the drug-binding tryptophan residue in LmrR, which is located in the C-terminal helix, is conserved in other PadR-s2 proteins, including those with known structure. However, in these latter proteins the equivalent tryptophans are buried in a completely closed dimer interface, making it highly unlikely that they have a similar ligand-binding role [9]. Unfortunately, assessment of the significance of the structural differences between LmrR and the other PadR-s2 proteins is prohibited by the lack of complete functional data.

To investigate whether LmrR is an exceptional member of the PadR-s2 family or whether its structural ligand-binding features are preserved in other members, requires structure/function analysis of LmrR homologs that function in multidrug or antibiotic resistance. Such a homolog of LmrR was recently identified in *Bacillus cereus* as the product of gene locus BC4206. Together with its neighboring gene BC4207, which encodes a putative membrane protein, BC4206 was shown to become highly upregulated if *B. cereus* is treated with low concentrations of enterocin AS-48, a broad-spectrum antimicrobial cyclic peptide produced by *Enterococcus faecalis* S-48 [13,14]. Here we report the crystal structure of the BC4206 gene product from *B. cereus* strain ATCC 14579, a subfamily-2 PadR-like protein which we named *bcPadR1*. In addition, we report the crystal structure of a *bcPadR1* homolog from *B. cereus* strain ATCC 10987, the product of gene locus BCE3449, which we named *bcPadR2*. This latter protein was selected for structural characterization because its gene is positioned in the vicinity of two genes encoding a putative antibiotic ABC efflux pump (gene loci BCE3447 and BCE3446). The proximity of these genes, similar as in the *lmrR-lmrCD* locus, could indicate that *bcPadR2* regulates the expression of the ABC efflux pump, perhaps following a similar ligand binding and induction mechanism as LmrR. Preliminary functional analysis, combined with our structural analysis and comparison with related proteins, reveal the roles of various conserved residues in the two subfamily-2 PadR-like proteins from *B. cereus*. Based on our results, we discuss possibilities for ligand-induced regulation of these proteins.

Materials and Methods

Cloning

The open reading frames encoding *bcPadR1* and *bcPadR2* were amplified by PCR from the genomic DNA of *Bacillus cereus* strains ATCC 14579 and ATCC 10987, respectively, and cloned in the vector pNSC8048 [15]. Plasmid pNSC8048 carries the *nisA* promoter, chloramphenicol selectable marker and a C-terminal strep-tag (SRWSHPQFEK). The forward and reverse primers for *bcpadR1* (locus BC4206) were 5'-CGACCATGGGCACAGC-

CAAATGTTAAAAGGTGTA-3' and 5'- GCTTCTA-GACTCCCCCTGTAATAAGTTATT-3', respectively, while forward and reverse primers for *bcpadR2* (locus BCE3449) were 5'-CGACCATGGAAAATTTAACTGAAATGCTGAAAG and 5'-GCTTCTAGAGTTTGACTTCAAGACGTTAAT-3', respectively. Those primers were designed to create NcoI/XbaI restriction sites of the resulting PCR products (shown as bold and underlined letters). The PCR fragments and pNSC8048 vector were digested with NcoI and XbaI restriction enzymes and the vector was dephosphorylated further with calf intestine alkaline phosphatase (CIAP, Fermentas). Ligation was performed using T4 ligase (Roche) to yield pNSC-*padR1* and pNSC-*padR2*. DNA sequences of the plasmids were all verified by sequencing (Macrogen, The Netherlands).

Expression and purification

To express *bcPadR1* and *bcPadR2*, plasmids pNSC-*padR1* and pNSC-*padR2* were transformed into *L. lactis* NZ9000 cells, which is a derivative of strain MG1363 carrying the *nisR/nisK* genes crucial for the induction and overexpression of the target protein under the nisin inducible system. The transformed *L. lactis* NZ9000 cells were grown in 100 ml of rich medium (M17, 0.5% glucose and 5 µg/mL chloramphenicol). After overnight growth at 30°C, the culture was transferred into 2 L of fresh media and grown also at 30°C. Overexpression was induced with 5 ng/mL nisin when cells were in the mid log phase (OD₆₀₀ of 0.6–0.8) and growth was continued for two hours. The cells were harvested by centrifugation (8000 rpm for 5 min at 4°C; JLA 10.500 rotor, Beckman), washed with 50 mM Tris-HCl, pH 7.4, and re-centrifuged (8000 rpm for 5 min at 4°C; 5810R rotor, Eppendorf). The pellets were stored at –20°C until further use.

For purification, the cell pellets were resuspended in lysis buffer, containing 100 mM Tris-HCl, pH 8.0, 150 mM NaCl, 1 mM EDTA, supplemented with 10 mg/ml lysozyme and a tablet of a Complete Protease Inhibitor cocktail (Roche). After 1 hour incubation at 30°C, MgSO₄ (10 mM) and DNaseI (10 µg/mL) were added into the suspension and incubation was continued for another 5 min. The cells were disrupted by sonication and remaining cell debris was removed by centrifugation (12,000 rpm for 10 min at 4°C; 5810R rotor, Eppendorf). *BcPadR1* or *bcPadR2* were purified from the supernatant using Streptactin Sepharose column chromatography, according to the protocol provided by the manufacturer (IBA Biotagnology GmbH). The protein-containing elution fractions (in 100 mM Tris-HCl, pH 8.0, 150 mM NaCl, 1 mM EDTA, 2.5 mM desthiobiotin) were diluted to 50 mM NaCl with buffer A (20 mM Tris-HCl, pH 8.0, 1 mM EDTA and 1 mM dithiothreitol) and then applied to a heparin column (5 ml Heparin FastFlow, GE Healthcare), connected to an ÄKTA Explorer FPLC system (GE Healthcare), to remove bound DNA from the protein. The retained protein was eluted by applying a linear gradient (2.5–100% in 15 column volumes) of 2 M NaCl in buffer A. The fractions containing *bcPadR1* or *bcPadR2* were pooled and concentrated to ~8 mg/ml in buffer containing 10 mM Tris-HCl, pH 8.0, 250 mM NaCl, 1 mM EDTA and 1 mM DTT using an Amicon Ultra 3 kDa cut-off concentrator (Millipore). The protein purity was confirmed by silver-stained SDS PAGE.

Expression of *bcPadR1* in *B. cereus* and determination of antimicrobial activity of AS-48

Plasmid pNSC-*padR1* was electroporated into *B. cereus* ATCC 14579 harboring the *nisRK* genes on plasmid pNZ9530 [16] and expression was induced with 20 ng/mL of nisin. The antimicrobial activity of AS-48 was determined as the minimal inhibitory

concentration (MIC) value against *B. cereus* following previous practice [17]. Bacterial growth was followed in the presence of various concentrations of AS-48 and monitored every 15 minutes using a TECAN GENios Absorbance Reader (TECAN). Without AS-48 addition, the final OD_{600 nm} value (at the end of the exponential phase) for the *B. cereus* culture was about 1.1±0.1. An inhibition curve was made by plotting OD_{600 nm} at the end of incubation versus AS-48 concentration. The minimal inhibitory concentration value was determined from the inhibition curve by interpolation. The lowest concentration of AS-48 at which less than 1% of the total increase in the OD₆₀₀, measured in the absence of AS-48, had occurred, was taken as the MIC value.

Electrophoretic mobility shift assay

Electrophoretic mobility shift assays (EMSAs) were carried out essentially as described by Susanna *et al* [18]. The promoter regions of *B. cereus* BC4206 and BC4029 genes were obtained by PCR with oligos (for BC4206, 5'-TTCAAGTGCCTTTGGTTC-3' and 5'-GATGCAACCTTCTAATAC-3'; for BC4029 5'-TTTGACGTTCTTCAAGC-3' and 5'-CTTTCAGCATTGACTTG-3') and the resulting fragments (250 bp and 347 bp for BC4206 and BC4029, respectively) were end-labeled with [γ -³²P]ATP using T4 polynucleotide kinase (Roche Nederland B.V., The Netherlands). Purified *bcPadR1* protein and its DNA probe were premixed on ice in binding buffer (20 mM Tris HCl (pH 8.0), 5 mM MgCl₂, 100 mM KCl, 0.5 mM dithiothreitol, 0.05 mg/ml poly(dI-dC), 0.05 mg/ml bovine serum albumin, and 8.7% glycerol) [18]. Reaction mixtures contained poly(dI-dC) that is known to eliminate non-specific DNA binding. Samples were incubated at 30°C, and were loaded on a 6% polyacrylamide gel after 20 min incubation. Gels were run in 1× TBE buffer (0.089 mM Tris, 0.089 mM boric acid, 0.022 mM EDTA) at 90 V for 60 minutes, dried in a vacuum dryer and autoradiographed using phosphoscreens and a Cyclone PhosphorImager (Packard Instruments, Meriden, CT).

Gel filtration. Analytical gel filtration was performed with a Superdex 200 PC 3.2/30 gel filtration column (GE Healthcare), mounted on a SMART-system (GE Healthcare). The running buffer contained 20 mM Tris-HCl, pH 8.0, 200 mM NaCl, 1 mM EDTA and 1 mM dithiothreitol. The injected protein samples volumes were 20 μ l. As molecular weight markers a mixture of five proteins was used: aldolase –158 kDa, bovine serum albumin –67 kDa, ovalbumin –43 kDa, chymotrypsin –25 kDa, and ribonuclease –13.7 kDa.

Crystallization. Prior to crystallization trials, *bcPadR1* was subjected to ThermoFluor-based stability optimization experiments [19] that were performed on a thermal cycler (myIQ, Bio-Rad) using Sypro-Orange dye (Invitrogen). The results revealed that *bcPadR1* was most stable in a buffer containing 20 mM MES pH 6.0, 250 mM NaCl, 1 mM EDTA and 1 mM DTT. Accordingly, both *bcPadR1* and *bcPadR2* were buffer exchanged to the aforementioned buffer using a PD-10 desalting column (GE Healthcare). The proteins were concentrated further to ~10 mg/ml and either used immediately for crystallization or stored at –80°C.

Initial crystallization trials were set up as vapour-diffusion sitting drops at 298 K using various commercially available screens [i.e., JCSG+ (Molecular Dimensions), Wizard Screen (Emerald Biosystem), Structure Screen (Emerald Biosystem) and Cryo Screen (Hampton Research)] and a Mosquito crystallization robot (TTP LabTech) for drop dispensing. Droplets were composed of 0.2 μ l protein stock solution and 0.2 μ l crystallization solution and were equilibrated against 60 μ l of the crystallization solution. Trigonal pyramid crystals of *bcPadR1* were obtained from JCSG+ Screen

condition no. 45, containing 0.17 M ammonium sulfate, 25.5% (w/v) PEG 4000 and 15% (v/v) glycerol. These crystals were used immediately for data collection without further optimization. For *bcPadR2*, similar crystals grew from JCSG+ condition no. 60 (0.1 M imidazole, pH 8.0, and 10% (w/v) PEG 8000) which was optimized manually using the hanging-drop vapour diffusion method. The final crystallization solution contained 0.1 M imidazole pH 8.0 and 9% (w/v) PEG 8000.

Data collection and structure determination. Prior to diffraction data collection, a single *bcPadR1* crystal with dimensions of ~160 μ m×160 μ m×180 μ m was transferred to a cryo-protectant solution containing 0.17 M ammonium sulfate, 27% (w/v) PEG 4000 and 20% (v/v) glycerol, and subsequently dipped into liquid nitrogen. A similar procedure was applied to a *bcPadR2* crystal (~100 μ m×100 μ m×160 μ m) with 0.1 M imidazole, pH 8.0, 10% (w/v) PEG 8000 and 20% (v/v) ethylene glycol as cryo-protectant. Diffraction data up to 2.5 Å and 2.2 Å resolution for *bcPadR1* and *bcPadR2*, respectively, were collected at 100 K using beam line ID14-2 at the ESRF, Grenoble, equipped with an ADSC Quantum 4 detector (see Table 1 for data collection statistics). The two data sets were indexed and integrated in space group *P4* with the program XDS [20], reindexed to space group *P422* and scaled and merged with the program Pointless and Scala [21], respectively, from the CCP4 software package [22]. Data collection statistics are shown in Table 1.

Table 1. Data collection and refinement.

	<i>bcPadR1</i>	<i>bcPadR2</i>
Data collection		
Wavelength (Å)	0.9330	0.9330
Space group	<i>P4</i> ₁ 2 ₁ 2	<i>P4</i> ₃ 2 ₁ 2
Unit cell dimensions (Å)	a = b = 73.5, c = 84.1	a = b = 43.9, c = 120.1
Resolution (Å)*	44–2.5 (2.64–2.5)	44–2.2 (2.32–2.2)
Total observations	65429	49981
Unique reflections	8474	6500
<I/σ>*	20.6 (2.9)	27.9 (3.3)
Completeness (%)*	100 (100)	99.7 (98.1)
R _{merge} *	0.074 (0.611)	0.042 (0.511)
Refinement		
Resolution (Å)	37–2.5	41–2.2
R-factor/R _{free} (%) [§]	20.2/22.6	22.3/27.7
Number of atoms		
Non-H protein	826	825
Water	17	17
Ligand	28 (glycerol, sulfate)	0
Average B (Å ²)	58.3	67.8
RMSD		
Bond lengths (Å)	0.003	0.010
Bond angles (°)	0.702	1.010
Ramachandran plot		
% most favoured	98.0	97.9
% disallowed	0.0	0.0

*Values in parentheses refer to the highest resolution shell.

[§]The R-factor is calculated for all measured reflections in the specified resolution range, while the R_{free} is calculated for reflections belonging to a random test set not used in refinement (10% of the data).

doi:10.1371/journal.pone.0048015.t001

The structures of *bcPadR1* and *bcPadR2* were solved by molecular replacement using the program Balbes [23] running on the YSBL web server (<http://www.ysbl.york.ac.uk/YSBLPrograms/>). The best solutions for the two proteins were found using the structure of a transcriptional regulator from *Enterococcus faecalis* V583 (PDB entry 3hhh) as a search model and by changing the space groups to $P4_12_12$ and $P4_32_12$ for *bcPadR1* and *bcPadR2*, respectively. The solutions were subjected to automated model building using ARP/wARP [24] via the ARP/wARP web service (<http://cluster.embl-hamburg.de/ARPwARP/remote-http.html>), and completed by applying several cycles of manual model building using COOT [25] and restrained-refinement using Phenix.refine [26]. TLS (Translation/Libration/Screw) parameters [27] were included in the final rounds of refinement, defining the HTH-domain and C-terminal helix as two separate TLS groups. The final models of *bcPadR1* and *bcPadR2* contain 103 residues (amino acids 3–105) and 99 residues (amino acids 3–66 and 72–106), respectively. The geometry of the models was validated by Molprobity [28].

Structure and sequence analysis. Structure and sequence analysis was carried out using the following software: SuperPose [29], for superimposition and calculation of root mean square deviations (RMSDs); ESPript [30] and Jalview (<http://www.jalview.org>) for preparation of sequence alignments; and Pymol (Schrödinger, LLC) for the depiction of structures and preparation of figures.

Accession numbers

Structure factors and the coordinates of the final models of *bcPadR1* and *bcPadR2* have been deposited in the Protein Data Bank (<http://www.rcsb.org>) with accession numbers 4ESB and 4ESF, respectively.

Results

Gene targets of *bcPadR1* and *bcPadR2*

Genes associated with resistance mechanisms that are transcriptionally controlled by PadR-like proteins are generally encoded in the vicinity of the *padR* genes. Figure 1A shows the chromosomal regions around the two *B. cereus padR* genes, in comparison to the *lmrR-lmrCD* operon. The gene encoding *bcPadR1* (locus BC4206 in *B. cereus* ATCC 14579) is located immediately downstream from BC4207, encoding a putative membrane protein of unknown function. These genes are predicted to share a common promoter, located immediately upstream from BC4206. Transcriptome analysis revealed that BC4206 and BC4207 are co-upregulated in response to enterocin AS-48 [14], indicating that these genes indeed form a bicistronic transcriptional unit. The same study also revealed that plasmid-based overexpression of BC4207 increased the resistance of *B. cereus* ATCC 14579 to AS-48, confirming the role of this gene in bacteriocin resistance, although its mechanism of operation is unknown. The BC4206-BC4207 transcriptional unit is conserved among *B. cereus* and *B. thuringiensis* species, but not present in the closely related *B. anthracis* [14]. To further examine the regulatory role of BC4206, we also overexpressed this gene in *B. cereus* ATCC 14579. Overexpression results in an increased sensitivity against AS-48 (MIC value of 1.0 µg/ml compared to a MIC value of 2.5 µg/ml for the wild-type strain, p -value < 0.005, >6 cultures as determined with Student's t -test) suggesting that *bcPadR1* acts as a repressor of the BC4206-BC4207 transcriptional unit, when AS-48 is not present in the medium. Electrophoretic mobility shift assays further reveal that purified *bcPadR1* specifically binds to the intergenic region between BC4205 and the BC4206-BC4207

operon (Figure 1B and 1C). Incubation of the DNA probe with 0.5 µM *bcPadR1* results in shifted bands, while higher *bcPadR1* concentration results in stronger, but more diffused binding (Figure 1C). This might indicate the binding of two or more *bcPadR1* dimers to the probe. The DNA probe used in these experiments contains the upstream regulatory region of BC4205 that codes for a putative spore photoproduct lyase. The expression of BC4205 is not altered in response to AS-48 addition [14], so its expression is likely to be unrelated to the AS-48 induced expression of BC4206-BC4207 operon. *In vitro* DNA binding of *bcPadR1* was not affected by the addition of AS-48 suggesting an indirect sensing of AS-48 in the medium, although we cannot exclude the possibility that slightly altered *in vitro* conditions (e.g. different binding buffer) are needed to observe any effect of AS-48 addition on DNA binding.

The gene encoding *bcPadR2* (locus BCE3449 in *B. cereus* ATCC 10987) lies downstream from two genes, BCE3447 and BCE3446, which encode a putative ABC-efflux pump. The product of BCE3447 forms the ATPase subunit of the transporter, while the product of BCE3446 forms the membrane permease. Interestingly, the amino acid sequence of the BCE3447-BCE3346 encoded pump is similar to that of the daunorubicin/doxorubicin resistance ABC transporter DrrAB from *Streptomyces peucetius* (overall sequence identity of 32%) [31,32]. The sequence identity of the BCE3447-BCE3346 encoded pump with LmrCD is 27%, but LmrCD is about twice as large as BCE3447-BCE3446 and DrrAB. DNA analysis indicates that the BCE3449 and BCE3447-BCE3346 genes do not share a common promoter, and are separated by another gene, BCE3448, which encodes a soluble protein of unknown function. The structure of the BCE3448-encoded protein has been solved by a structural genomics consortium (PDB entry 2O3L) and shows a left-handed superhelix fold containing 5 α -helices. Genomic analysis reveals that the BCE3449-BCE3448-BCE3447-BCE3446 gene organization is conserved in various *Bacillus* species, but without functional expression data we cannot confirm that these genes form an operon or are coregulated.

Sequence analysis

BcPadR1 and *bcPadR2* contain 105 and 106 amino acid residues, respectively, and have all the characteristics of the PadR-s2 protein family. Figure 2 shows a multiple sequence alignment of the two proteins with other PadR-s2 proteins of which structures are currently deposited in the PDB, including LmrR. Pair-wise sequence identities range from 20% (*bcPadR2* compared with a transcriptional regulator from *Clostridium thermocellum*, PDB entry 1XMA) to 61% (*bcPadR2* compared with a transcriptional regulator from *Enterococcus faecalis* V583, PDB entry 3HHH). *BcPadR1* and *bcPadR2* share a sequence identity of 45%, and are 26% and 30% identical in sequence to LmrR, respectively. Using an alignment-derived profile hidden Markov model, all homologs of *bcPadR1* and *bcPadR2* currently deposited in the Uniprot database were identified (>2150 sequences) and used to derive conserved sequence motifs. The highly conserved residues of the PadR-s2 proteins are mainly located in the wHTH domain and cluster in three regions, (i) at the N-terminus of helix $\alpha 2$ [motif YGYE(I/L)], (ii) in helix $\alpha 3$ [motif EGT(L/I)YPxLxRLE] and (iii) in the region encompassing strand $\beta 2$ of the wing and the N-terminus of helix $\alpha 2$ [motif G(P/R)RKYYx(L/I)TxXG]. The identified sequence motifs partly overlap with the consensus sequence previously derived for all PadR-like proteins [4]. In addition to the above mentioned conserved sequence motifs, other highly conserved residues are found in more isolated positions at the N-terminus, helix $\alpha 1$ and the C-terminal helix of the subfamily

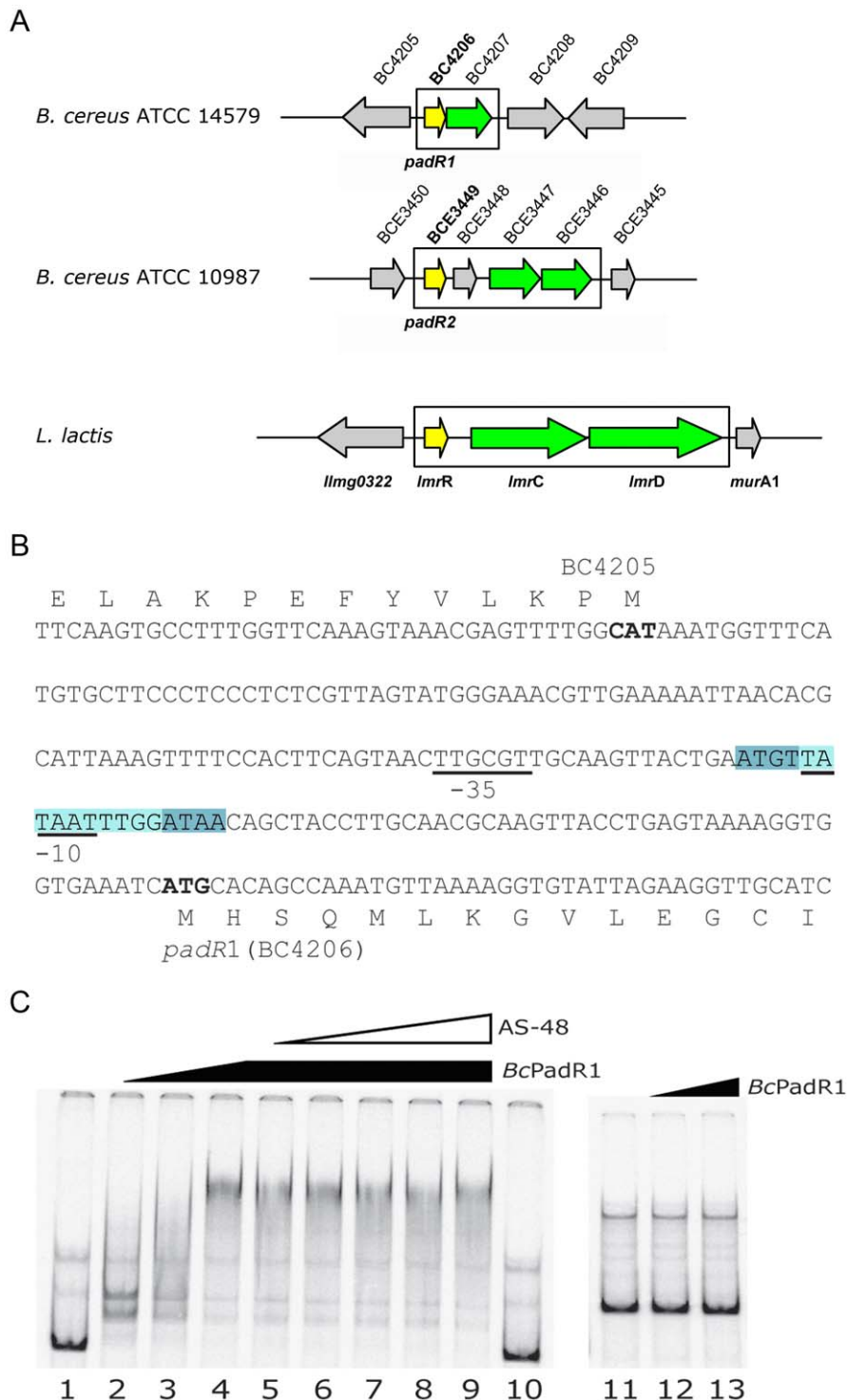


Figure 1. Genomic neighborhood of the *bcPadR1* and *bcPadR2* encoding genes and analysis of promoter binding. (A) Organization of the BC4206(*bcPadR1*)-BC4207 operon of *B. cereus* ATCC 14579, the putative BCE3449(*bcPadR2*)-BCE3448-BCE3447-BCE3446 regulon of *B. cereus* ATCC 10987 and the *lmrR-lmrCD* regulon of *L. lactis*. The relative scale of the genes and intergenic regions is proportional to nucleotide length. Boxes indicate the operon/regulon boundaries. The PadR-encoding genes are colored in yellow, while their (putative) target genes, encoding resistance-associated membrane proteins, are in green. (B) The sequence of the intergenic region between BC4205 and BC4206 that is used for the EMSA experiments. Putative -35 and -10 promoter sequences of BC4206 are underlined, the start codons of BC4205 and BC4206 are highlighted in bold, and the amino acids of the coded proteins are indicated above the DNA sequence. The putative binding site of *bcPadR1* (homologous to the canonical ATGT/ACAT inverted sequence motif) is highlighted in blue. (C) EMSA experiments with *bcPadR1*. DNA fragments encompassing the promoter regions of BC4206 (lanes 1–10) and BC4209 (lanes 11–13, negative control) were prepared by PCR and end labeled with ^{33}P . DNA binding was assayed as described in the Materials and Methods. Lanes 1, 10 and 11 contain the free DNA probe. Samples run on lanes 2 and 12 contain 0.5 μM ; lane 3 1 μM ; lanes 4–9 and 13 2 μM of purified *bcPadR1* protein. Lanes 5 to 9 contain samples including increasing concentrations of AS-48 from 0.5 pM to 0.69 μM . doi:10.1371/journal.pone.0048015.g001

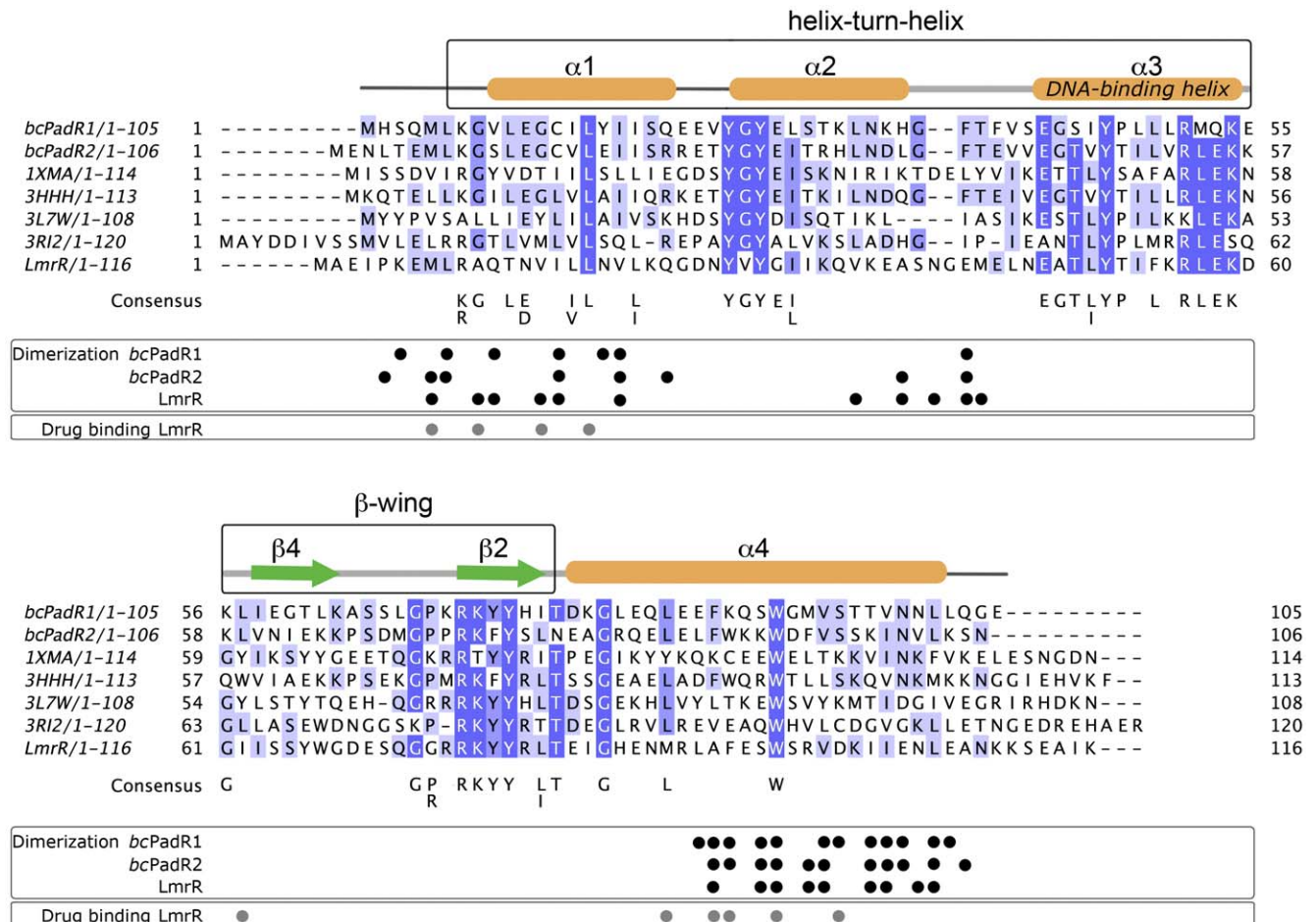


Figure 2. Multiple sequence alignment of *bcPadR1*, *bcPadR2*, and other members of the PadR-s2 subfamily. Only sequences for which structures are available in the PDB are shown in the alignment. The PadR-s2 proteins with unpublished structures are addressed by their PDB entry names: 1XMA, a putative transcriptional regulator from *Clostridium thermocellum*; 3HHH, a putative transcriptional regulator from *Enterococcus faecalis* V583; 3L7W, uncharacterized protein SMU.1704 from *Streptococcus mutans* UA159; 3RI2, a putative transcriptional regulator from *Eggerthella lenta* DSM 2243. Residues that participate in dimerization (for *bcPadR1*, *bcPadR2*, and *LmrR*) and/or have a role in drug binding (only for *LmrR*) are indicated by small spheres below the sequences. The consensus sequence is derived from a multiple sequence alignment of 2156 PadR-s2 proteins using as criteria that the conserved residue(s) should be present in at least 50% of the sequences.
doi:10.1371/journal.pone.0048015.g002

2 PadR-like proteins, including the central tryptophan residue in the C-terminal helix which has a central role in multidrug-binding in *LmrR*.

Structure determination

To allow easy production of pure protein for crystallization, *bcPadR1* and *bcPadR2* were expressed with a C-terminal streptavidin-tag (SRWSHPQFEK) using an *L. lactis* nisin-overexpression system. Protein purification was carried out in two steps using Strep-Tactin and DNA affinity chromatography. Gel filtration experiments revealed that the recombinant *bcPadR1* and *bcPadR2* proteins have an apparent molecular weight of ~43 kDa, similar as observed previously for *LmrR* and consistent with the presence of elongated dimers in solution (the calculated molecular weight of monomeric strep-tagged *bcPadR1* and *bcPadR2* is 13.3 kDa and 13.7 kDa, respectively)

BcPadR1 was crystallized in space group $P4_12_12$, with one protein molecule per asymmetric unit and a solvent content of 71%. Similarly, *bcPadR2* was crystallized in space group $P4_32_12$, with one protein molecule per asymmetric unit and a solvent content of 42%. The *bcPadR* structures were determined by

molecular replacement using the structure of the PadR-like protein from *E. faecalis* V583 as a search model. Model building and refinement were somewhat hampered by relatively high atomic displacement parameters (B-factors), indicative of some global disorder or flexibility of the proteins, even though the overall fit to the electron density is well defined. The final refined structures of *bcPadR1* and *bcPadR2* have an R-factor/ R_{free} of 20.2/22.6% at 2.5 Å resolution and 22.3/27.7% at 2.2 Å resolution, respectively, with good geometry (see Table 1 for details of the refinement statistics). The two structures are highly similar with a α -backbone root mean square deviation (RMSD) of 1.45 Å (for 96 common residues). The N-termini (residues 1–2 in both *bcPadR* proteins) and the C-terminal strep-tags (residues 106–115 in *bcPadR1* and residues 108–116 in *bcPadR2*) were not included in the models due to weak or absent electron density. In addition, residues 67–71 in the β -wing of *bcPadR2* were found to be disordered and therefore left out from the model.

Overall structures of *bcPadR1* and *bcPadR2*

In the crystals, *bcPadR1* and *bcPadR2* form similar dimers, with a dimeric 2-fold axis that coincides with a crystallographic 2-fold

axis. The approximate dimensions of the dimers are $80 \text{ \AA} \times 34 \text{ \AA} \times 30 \text{ \AA}$ (Figure 3A). The *bcPadR1* and *bcPadR2* subunits contain a typical wHTH DNA-binding domain, consisting of helices $\alpha 1$, $\alpha 2$, the DNA recognition helix $\alpha 3$ and strands $\beta 1$ and $\beta 2$ (together forming the wing), and a dimerization domain, including the C-terminal helix $\alpha 4$. Helix $\alpha 4$ forms a protruding arm which in the dimer interacts with helices $\alpha 4'$ and $\alpha 1'$ of the dimer-mate. Dimerization of *bcPadR1* and *bcPadR2* buries approximately 1740 \AA^2 solvent-accessible surface area per subunit which is related to $\sim 30\%$ of the total surface area. The dimeric interface involves mainly van der Waals contacts between hydrophobic residues, most of which are conserved between the two *bcPadR* proteins (see Figure 2). In addition a few hydrogen bonds are observed at the dimer interface, but these are not conserved.

BcPadR1 and bcPadR2 show a closed dimeric interface

Although similar in overall fold, it is evident that the two *bcPadR* structures do not show the same dimeric interface as LmrR (Figures 3 and 4). Unlike LmrR, but like the other PadR-s2 proteins with known structure, the *bcPadR1* and *bcPadR2* dimers have a completely closed dimer interface. The differences at the dimer interface are associated with changes in the relative orientation of helices $\alpha 1$ and $\alpha 4$ with respect to the core of the wHTH domain (Figure 4B). In addition, helix $\alpha 4$ in *bcPadR1* and *bcPadR2* shows significant bending towards the dimeric centre, whereas the equivalent helix in LmrR is almost perfectly straight

(Figure 4C). As a consequence, helices $\alpha 4$ and $\alpha 4'$ in the *bcPadR* dimers can approach each other closely at the dimer interface, allowing a coiled-coil interaction mode. In LmrR the C-terminal helices do not make any mutual contacts, but, instead, interact strongly with helices $\alpha 1$ and $\alpha 2$ of the dimer mate. Intriguingly, despite these significant differences in dimeric organization, the residues in *bcPadR* proteins and LmrR that form the inter-subunit interactions are located at similar positions in the structures (Figure 2). It is unclear how the differences in amino acid sequence at these regions affect the conformation of the polypeptides in the dimer. In particular, the highly conserved tryptophan residues in the C-terminal helices of the *bcPadR* dimers (Trp91/Trp91' and Trp93/Trp93' in *bcPadR1* and *bcPadR2*, respectively), which are the equivalent of Trp96/Trp96' in LmrR, are completely buried in the dimer interface. The closed dimer conformation and inaccessibility of the conserved tryptophan residues of the *bcPadR* proteins are incompatible with a drug-binding mechanism as observed in LmrR.

Structural similarity with non-PadR-like transcription factors

A structural similarity search against available structures in the Protein Data Bank (PDB) using the DALI server [33] reveals that *bcPadR1* and *bcPadR2* are not only similar to other PadR-like proteins, but also to various non-PadR-like transcription factors including members of the MarR family, SmtB/ArsR family and the MecI/BlaI family (Table 2). These proteins all contain

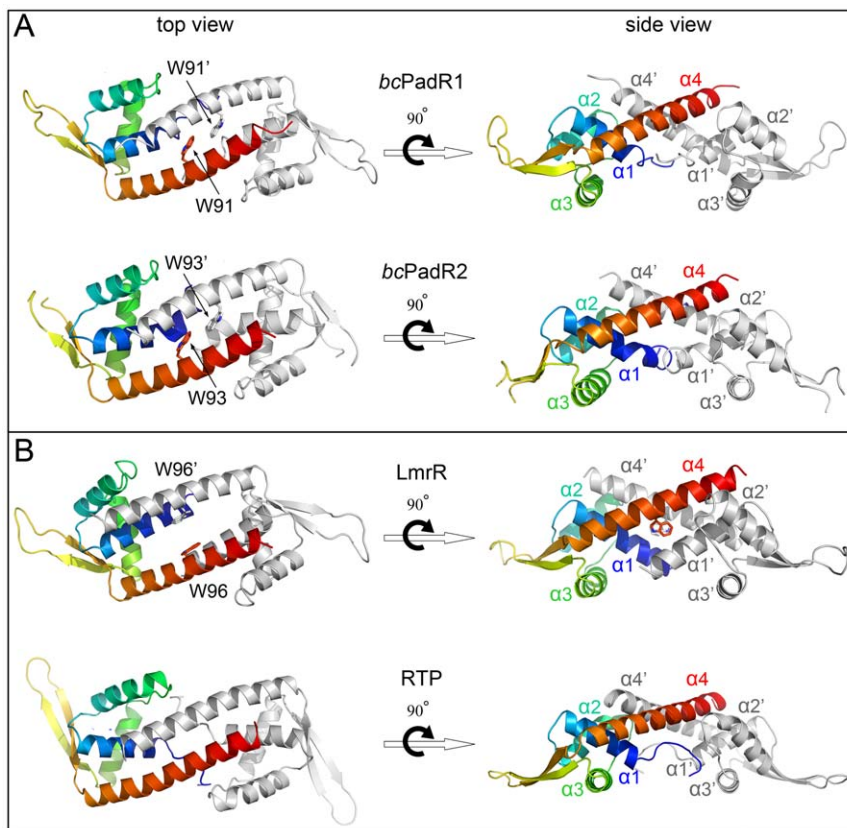


Figure 3. Ribbon representations of the *bcPadR* dimers and selected structural homolog. (A) *bcPadR1*, (B) *bcPadR2*, (C) LmrR (PDB code 3F8B), and (D) RTP, a replication terminator protein from *Bacillus subtilis* (PDB code 1F4K). For each dimer, one of the subunits is shown in a rainbow color gradient from the N-terminus (blue) to the C-terminus (red), whereas the other subunit is colored grey. Helices involved in dimerization are indicated. Residues Trp91 of *bcPadR1*, Trp93 of *bcPadR2*, and Trp96 of LmrR are drawn in stick representation. doi:10.1371/journal.pone.0048015.g003

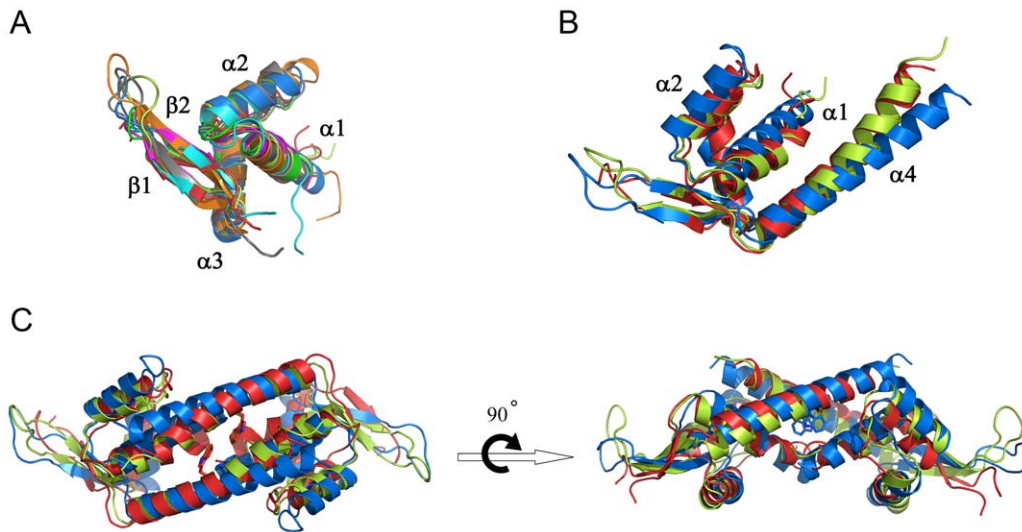


Figure 4. Structural comparison between *bcPadR1*, *bcPadR2* and LmrR. (A) Superpositions of the wHTH domains of *bcPadR1* (light-green), *bcPadR2* (red), LmrR (blue), and the following homologs: MexR (green), SmtB (magenta), Blal (cyan), RTP (orange), and Pex (gray) with the secondary structure elements indicated and labeled. (B) Superposition of the single *bcPadR1*, *bcPadR2* and LmrR subunits. (D) Superposition of the *bcPadR1*, *bcPadR2* and LmrR dimers.

doi:10.1371/journal.pone.0048015.g004

wHTH-domains for DNA binding and form functional dimers. The similarities of the non-PadR-like structural homologs of *bcPadR1* and *bcPadR2* are mainly limited to the wHTH domains, which can be superimposed to those of *bcPadR1* and *bcPadR2* with RMSDs (for C α -backbone superpositions) of 1.1–1.9 Å (Figure 4A). In contrast, the dimerization topologies of the non-PadR-like structural homologs of *bcPadR1* and *bcPadR2* are highly diverse, often including additional helices at the N- and C-terminal regions. One notable exception is the transcription factor RTP (replication terminator protein) from *Bacillus subtilis*, which plays a crucial role in the coordinated termination of DNA replication [34]. Despite the absence of significant sequence homology, *bcPadR1* and *bcPadR2* show a highly similar overall topology and dimeric organization as RTP, including the presence of a single C-terminal helix for dimerization (Figure 3). The striking similarities

of the *bcPadR* and RTP structures strongly suggest that these proteins use a common mode of DNA binding.

Putative DNA-binding interactions

To understand how *bcPadR1* and *bcPadR2* may bind to DNA, the *bcPadR* structures were superimposed to structures of close homologs in complex with DNA (Figure 5). At present no structure is available of a PadR-like protein bound to its cognate DNA. However, DNA-bound structures are available for two of the non-PadR-like close homologs identified by the DALI search, i.e., the replication terminator protein RTP (PDB entry 1F4K) and the transcriptional repressor BlalI (PDB entry 1XSD) [34,35]. RTP and BlalI exploit common principles to fulfill their role as DNA-binding regulatory proteins, which most probably are also used by the *bcPadR* proteins. The operator sequences of RTP and BlalI

Table 2. DALI-identified structural homologs of *bcPadR1* and *bcPadR2*.*

<i>bcPadR1/bcPadR2</i>								
PDB-ID	Z-score	RMSD (Å)	C α aligned	Nr. res	% id.	Protein name	Protein family	Ref.
3HHH	16.1/17.7	1.6/1.7	101/101	103/103	42/61	n.k.	PadR-s2	u.
3L7W	14.2/13.6	2.0/2.7	99/100	106/106	27/27	n.k.	PadR-s2	u.
3RI2	14.0/14.0	2.5/1.6	99/100	112/112	30/26	n.k.	PadR-s2	u.
1XMA	13.9/14.8	2.6/1.5	97/98	103/101	22/20	n.k.	PadR-s2	u.
1LNW	12.8/12.0	2.7/3.0	93/88	141/141	13/16	MexR	MarR	[40]
3F8B	12.5/11.7	3.1/2.7	100/98	105/101	23/30	LmrR	PadR-s2	[9]
1YG2	11.0/10.6	3.2/2.8	83/82	169/169	22/24	AphA	PadR-s1	[8]
1F4K	10.6/11.0	3.1/2.5	98/98	115/115	12/15	RTP	RTP	[34]
1SMT	10.1/9.5	2.6/2.9	78/77	98/101	14/19	SmtB	SmtB/ArsR	[41]
1SD6	9.7/9.6	3.3/3.1	84/84	119/119	15/19	BlalI	MecI/BlalI	[35]
2E1N	9.3/9.1	3.5/3.1	90/89	112/112	21/25	Pex	PadR-s1	[7]

Abbreviations: PadR-s1, PadR-like subfamily-1; PadR-s2, PadR-like subfamily-2, n.k., not known; u, unpublished.

*The DALI-search was performed using a single subunit of each *bcPadR* dimer.

doi:10.1371/journal.pone.0048015.t002

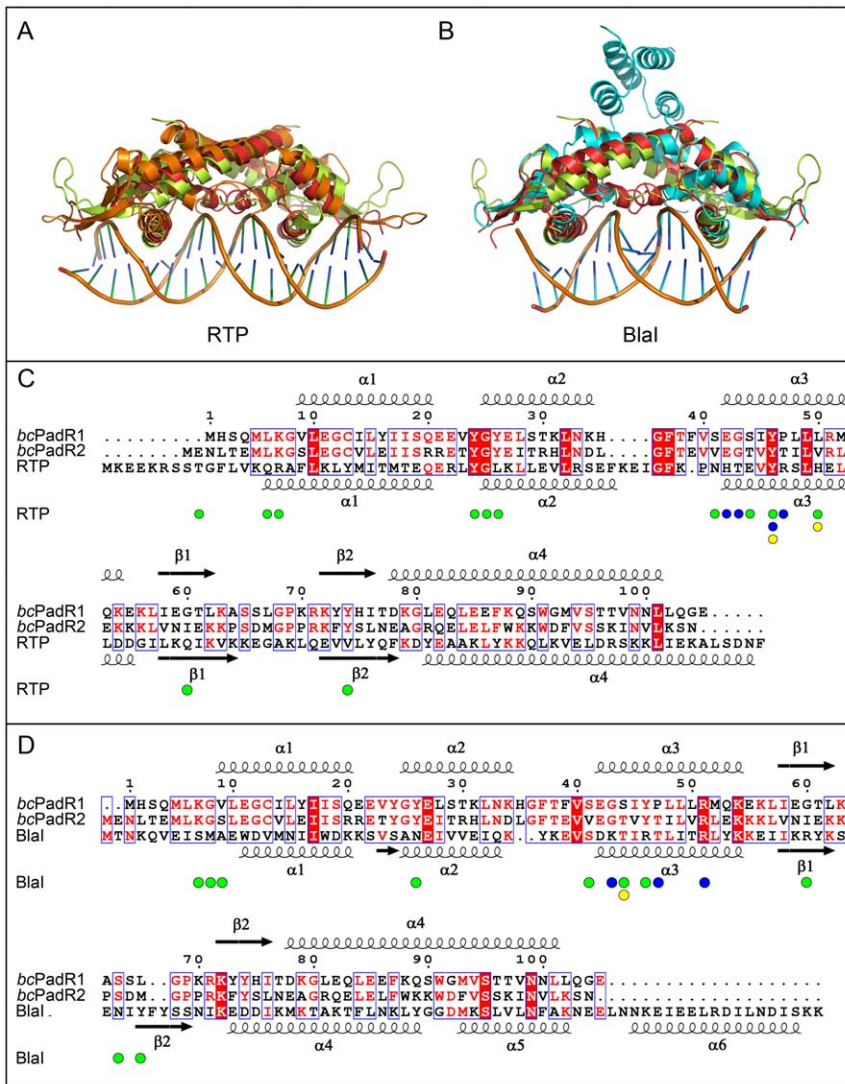


Figure 5. Modeling of the DNA-bound *bcPadR* complexes. (A) Superposition of the *bcPadR1* (light-green) and *bcPadR2* (red) dimers onto DNA-bound RTP (orange, PDB code 1F4K). (B) Superposition of the *bcPadR1* (light-green) and *bcPadR2* (red) dimers onto DNA-bound BlaI (cyan, PDB code 1XSD). Below the superpositions are structure-based sequence alignments including secondary structures. Residues of RTP and BlaI which participate in DNA binding are indicated with small spheres using the following color scheme: green, interacting with the phosphate backbone; blue, interacting with the base moiety and yellow, interacting with the ribose backbone. doi:10.1371/journal.pone.0048015.g005

contain specific inverted repeat motifs and the proteins bind such that their dimeric dyads are aligned with the inverted repeat dyads of the DNA operators. In this way, the recognition helices ($\alpha 3$) of the dimer-related wHTH domains can insert into two successive major grooves of the DNA, while the β -wings lie across the phosphate backbone, within the vicinity of adjacent minor groove clefts. DNA binding is stabilized by electrostatic interactions between the highly positively charged surface of the DNA binding site and the negatively charged DNA backbone. Additional DNA:protein interactions comprise various non-bonding contacts, including hydrophobic interactions, and a few hydrogen bond interactions. Residues in the $\alpha 3$ -helix are responsible for specific DNA binding and recognition of the operator DNA sequence, by penetrating into the major groove and forming hydrogen bonds with bases of the nucleotides.

The *bcPadR1* dimer can be superimposed to the DNA-bound complexes of RTP and BlaI with RMSD values of 3.5 Å (for 176

common C α atoms divided equally between both subunits) and 4.1 Å (for 153 common C α atoms), respectively. Likewise, the *bcPadR2* dimer can be fitted to the DNA-bound complexes of RTP and BlaI with RMSD values of 2.9 Å (for 179 common C α atoms) and 3.4 Å (for 155 common C α atoms). Overall, the dimers of *bcPadR1* and *bcPadR2* are highly similar to RTP and BlaI, but there are small differences in the relative dispositions of the dimer-related subunits which affect the relative orientations of the $\alpha 3$ helices. Since DNA-binding by transcription factors is often associated with specific conformational changes in both protein and DNA, the superpositions cannot be used to accurately predict the details of the DNA binding mechanism of *bcPadR1* and *bcPadR2*. However, analysis of the models in combination with a structure-based sequence alignment of *bcPadR1*, *bcPadR2*, RTP and BlaI (Figure 5) leads to a few interesting observations. First, like in RTP and BlaI, the complementary surfaces in *bcPadR1* and *bcPadR2* that form the putative DNA binding sites are highly

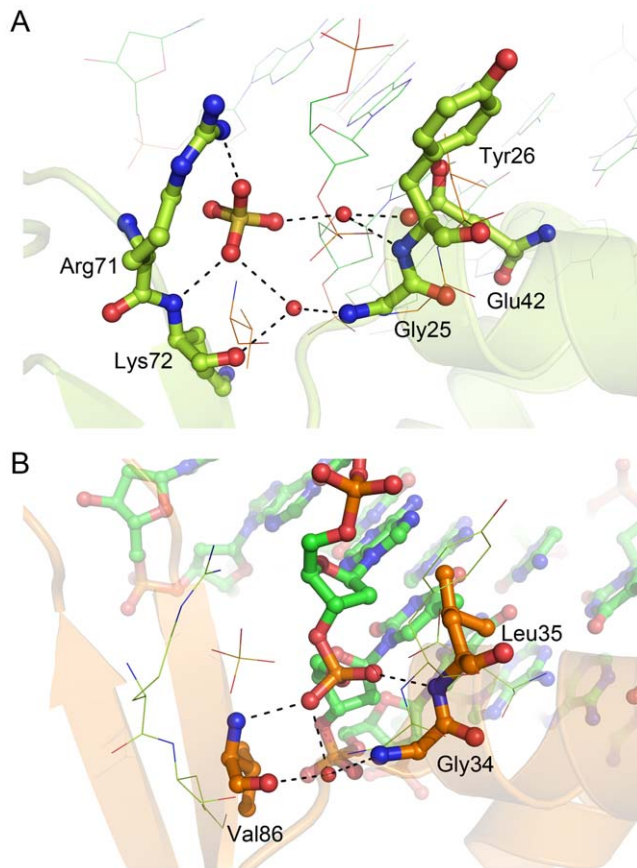


Figure 6. The bound sulfate anion in the *bcPadR1* structure. (A) Interactions between *bcPadR1* residues and the sulfate ion. Also shown is the DNA-bound RTP structure (PDB entry 1F4K) onto which the *bcPadR1* dimer was superimposed. The *bcPadR1* residues and the sulfate ion are shown in ball-and-stick representation and labeled, while the DNA strand of the RTP-DNA complex is drawn using lines. (B) Interactions between the RTP residues and the DNA phosphate backbone adjacent to the sulfate anion in the superimposed *bcPadR1* structure. The RTP residues and DNA strands are shown in ball-and-stick representation and labeled, while the *bcPadR1* residues and sulfate are drawn using lines.
doi:10.1371/journal.pone.0048015.g006

positively charged, due to the presence of various lysine and arginine residues. A number of these lysine and arginine residues from part of the previously described conserved sequence motifs in the PadR-s2 proteins, in particular those located in helix $\alpha 3$ and the β -wing, strongly implying a direct role in DNA binding. Furthermore, the conserved YGYE motif in *bcPadR1* and *bcPadR2*, which is located at the N-terminal end of helix $\alpha 2$, is partly preserved in RTP (residues 33–36 with sequence YGLK). In RTP, the side chain of Tyr33, together with the backbone amides of Gly34 and Leu35, forms hydrogen bonds with the phosphate-backbone of the DNA. As these interactions are crucial for the strong DNA binding affinity of RTP [36], it is likely that the conserved residues in *bcPadR1* and *bcPadR2* have a similar DNA binding role. This is corroborated by the observation of a bound sulfate anion in the *bcPadR1* structure, which forms interactions with the highly conserved residues Gly25, Tyr26, Glu42 Arg71, and Lys72, likely mimicking the interactions with a phosphate moiety of the DNA backbone (Figure 6). Finally, the $\alpha 3$ helices of the *bcPadR* proteins show a limited number of conserved residues relative to the equivalent helices in RTP and BlaI. Interestingly,

two residues of the conserved EGTLYP \times LxRLE motif are identical to sequence-specific DNA binding residues in RTP or BlaI, i.e., Tyr46 and Arg51, strongly suggesting that these residues in helix $\alpha 3$ of the *bcPadR* proteins have a similar DNA binding role. However, the limited overall sequence conservation of the $\alpha 3$ helices is also indicative of the differences that must exist between the specific cognate operator sequences of these DNA-binding proteins.

Discussion

In this study, we have determined the crystal structures of *bcPadR1* and *bcPadR2*, which are the products of gene loci BC4206 and BCE3449 of *B. cereus* strains ATCC 14579 and ATCC 10987, respectively. Functional data point toward the hypothesis that *bcPadR1* autoregulates the transcription of its own gene, as *bcPadR1* binds to the promoter region of gene BC4206 and overexpression of BC4206 gene results in increased sensitivity against AS-48. The structures of *bcPadR1* and *bcPadR2* are similar to LmrR, containing a conserved N-terminal wHTH DNA binding domain and a C-terminal helix involved in dimerization. The conserved structures and sequence relationships confirm that all three proteins belong to the same subfamily of small PadR proteins (subfamily 2 according to Huillet et al. [4], which we abbreviated as PadR-s2.) The identification of conserved sequence motifs in the wHTH domains, in particular in the $\alpha 3$ DNA recognition helix, further suggests that the PadR-s2 proteins share a common cognate DNA operator sequence. Operator sites of LmrR in the *lmrR* and *lmrCD* promoter regions have been identified previously [5,12], and were shown to contain an ATGT/ACAT inverted sequence motif, separated by a short spacer of about 8–10 nucleotides. The inverted repeat is identical to the conserved DNA sequence motif revealed for members of the other subfamily of PadR proteins (PadR-s1 family) [1,37]. Indeed, similar sequence motifs, although somewhat degenerate, are present in the promoter of the BC4206–4207 operon [ATGT-(N)₁₀-ATAA, Figure 1B] and the putative promoter region preceding BCE3449 [CTGT-(N)₈-ATAT, data not shown]. Functional studies and footprinting analysis are required to fully establish the identity of the target DNA operator sites and to identify other possible target genes controlled by *bcPadR1* and *bcPadR2*.

Compared to related transcription factors of the MarR, SmtB/ArsR and MecI/BlaI families, the *bcPadR* proteins show a “minimal” fold, lacking extra N- and C-terminal helices associated with dimerization. In the non-PadR-like proteins the extra helices often play a role in the mechanisms of transcriptional induction, allowing modulation of DNA binding activities through direct binding of a ligand. Also the structural features in LmrR that are related with its role as a multi-drug induced transcription regulator, i.e., a large central pore with two opposing tryptophan residues for multi-drug binding, are notably absent in *bcPadR1* and *bcPadR2*. These observations suggest that the DNA binding activities of *bcPadR1* and *bcPadR2* are not directly modulated by ligands. In line with this hypothesis, *in vitro* DNA binding of *bcPadR1* was not altered by the presence of AS-48. This is not surprising since AS-48 is known to target the cell membrane, inducing membrane pore formation [14], and is unlikely to enter the cytoplasm. Perhaps, the *bcPadR* proteins undergo a conformational change, which opens the dimer interface, thereby forming a ligand binding site. Alternatively, transcriptional regulating by the *bcPadR* proteins may involve an indirect induction mechanism with the participation of another protein. Such a mechanism has been proposed for the phenolic acid stress

response in *L. plantarum*, which is regulated by the founding member of the PadR-like transcription factors and involves a protein belonging to the universal stress protein family [38,39]. Examining such possibilities for the mechanism of action of the *bc*PadR proteins has to await experimental data characterizing their regulatory functions and identifying the target genes which they control.

References

- Gury J, Barthelmebs L, Tran NP, Divies C, Cavin JF (2004) Cloning, deletion, and characterization of PadR, the transcriptional repressor of the phenolic acid decarboxylase-encoding padA gene of *Lactobacillus plantarum*. *Appl Environ Microbiol* 70: 2146–2153.
- Tran NP, Gury J, Dartois V, Nguyen TKC, Seraut H, et al. (2008) Phenolic acid-mediated regulation of the *padC* gene, encoding the phenolic acid decarboxylase of *Bacillus subtilis*. *J Bacteriol* 190: 3213–3224.
- Kovacikova G, Lin W, Skorupski K (2003) The virulence activator AphA links quorum sensing to pathogenesis and physiology in *Vibrio cholerae* by repressing the expression of a penicillin amidase gene on the small chromosome. *J Bacteriol* 185: 4825–4836.
- Huillet E, Velge P, Vallaeys T, Pardon P (2006) LadR, a new PadR-related transcriptional regulator from *Listeria monocytogenes*, negatively regulates the expression of the multidrug efflux pump MdrL. *FEMS Microbiol Lett* 254: 87–94.
- Agustiandari H, Lubelski J, van den Berg van Saparoea HB, Kuipers OP, Driessen AJM (2008) LmrR is a transcriptional repressor of expression of the multidrug ABC transporter LmrCD in *Lactococcus lactis*. *J Bacteriol* 190: 759–763.
- Takai N, Ikeuchi S, Manabe K, Kutsuna S (2006) Expression of the circadian clock-related gene *peixin* cyanobacteria increases in darkness and is required to delay the clock. *J Biol Rhythms* 21: 235–244.
- Arita K, Hashimoto H, Igari K, Akaboshi M, Kutsuna S, et al. (2007) Structural and biochemical characterization of a cyanobacterium circadian clock-modifier protein. *J Biol Chem* 282: 1128–1135.
- De Silva RS, Kovacicova G, Lin W, Taylor RK, Skorupski K, et al. (2005) Crystal structure of the virulence gene activator AphA from *Vibrio cholerae* reveals it is a novel member of the winged helix transcription factor superfamily. *J Biol Chem* 280: 13779–13783.
- Madoori PK, Agustiandari H, Driessen AJM, Thunnissen AMWH (2009) Structure of the transcriptional regulator LmrR and its mechanism of multidrug recognition. *EMBO J* 28: 156–166.
- Alekshun MN, Levy SB, Mealy TR, Seaton BA, Head JF (2001) The crystal structure of MarR, a regulator of multiple antibiotic resistance, at 2.3 Å resolution. *Nat Struct Biol* 8: 710–714.
- Lubelski J, de Jong A, van Merkerk R, Agustiandari H, Kuipers OP, et al. (2006) LmrCD is a major multidrug resistance transporter in *Lactococcus lactis*. *Mol Microbiol* 61: 771–781.
- Agustiandari H, Peeters E, de Wit JG, Charlier D, Driessen AJM (2011) LmrR-mediated gene regulation of multidrug resistance in *Lactococcus lactis*. *Microbiology* 157: 1519–1530.
- Maqueda M, Galvez A, Bueno MM, Sanchez-Barrena MJ, Gonzalez C, et al. (2004) Peptide AS-48: Prototype of a new class of cyclic bacteriocins. *Curr Protein Pept Sci* 5: 399–416.
- Grande Burgos MJ, Kovacs AT, Mironczuk AM, Abriouel H, Galvez A, et al. (2009) Response of *Bacillus cereus* ATCC 14579 to challenges with sublethal concentrations of enterocin AS-48. *BMC Microbiol* 9: 227.
- Lubelski J, Mazurkiewicz P, van Merkerk R, Konings WN, Driessen AJ (2004) *ydaG* and *ydbA* of *Lactococcus lactis* encode a heterodimeric ATP-binding cassette-type multidrug transporter. *J Biol Chem* 279: 34449–34455.
- Kleerebezem M, Beerthuyzen MM, Vaughan EE, de Vos WM, Kuipers OP (1997) Controlled gene expression systems for lactic acid bacteria: Transferable nisin-inducible expression cassettes for *Lactococcus*, *Leuconostoc*, and *Lactobacillus* spp. *Appl Environ Microbiol* 63: 4581–4584.
- Kuipers OP, Rollema HS, Yap WM, Boot HJ, Siezen RJ, et al. (1992) Engineering dehydrated amino acid residues in the antimicrobial peptide nisin. *J Biol Chem* 267: 24340–24346.
- Susanna KA, van der Werff AF, den Hengst CD, Calles B, Salas M, et al. (2004) Mechanism of transcription activation at the comG promoter by the competence transcription factor ComK of *Bacillus subtilis*. *J Bacteriol* 186: 1120–1128.
- Ericsson UB, Hallberg BM, DeTitta GT, Dekker N, Nordlund P (2006) Thermofluor-based high-throughput stability optimization of proteins for structural studies. *Anal Biochem* 357: 289–298.
- Kabsch W (2010) Integration, scaling, space-group assignment and post-refinement. *Acta Crystallogr D Biol Crystallogr* 66: 133–144.
- Evans P (2006) Scaling and assessment of data quality. *Acta Crystallogr D Biol Crystallogr* 62: 72–82.
- Winn MD, Ballard CC, Cowtan KD, Dodson EJ, Emsley P, et al. (2011) Overview of the CCP4 suite and current developments. *Acta Crystallogr D Biol Crystallogr* 67: 235–242.
- Long F, Vagin AA, Young P, Murshudov GN (2008) BALBES: A molecular-replacement pipeline. *Acta Crystallogr D Biol Crystallogr* 64: 125–132.
- Langer G, Cohen SX, Lamzin VS, Perrakis A (2008) Automated macromolecular model building for X-ray crystallography using ARP/wARP version 7. *Nat Protoc* 3: 1171–1179.
- Emsley P, Lohkamp B, Scott WG, Cowtan K (2010) Features and development of coot. *Acta Crystallogr D Biol Crystallogr* 66: 486–501.
- Adams PD, Afonine PV, Bunkoczi G, Chen VB, Davis IW, et al. (2010) PHENIX: A comprehensive python-based system for macromolecular structure solution. *Acta Crystallogr D Biol Crystallogr* 66: 213–221.
- Winn MD, Isupov MN, Murshudov GN (2001) Use of TLS parameters to model anisotropic displacements in macromolecular refinement. *Acta Crystallogr D Biol Crystallogr* 57: 122–133.
- Chen VB, Arendall WB 3rd, Headd JJ, Keedy DA, Immormino RM, et al. (2010) MolProbity: All-atom structure validation for macromolecular crystallography. *Acta Crystallogr D Biol Crystallogr* 66: 12–21.
- Krisinel E, Henrick K (2004) Secondary-structure matching (SSM), a new tool for fast protein structure alignment in three dimensions. *Acta Crystallogr D Biol Crystallogr* 60: 2256–2268.
- Gouet P, Robert X, Courcelle E (2003) ESPript/ENDscript: Extracting and rendering sequence and 3D information from atomic structures of proteins. *Nucleic Acids Res* 31: 3320–3323.
- Kaur P (1997) Expression and characterization of DrrA and DrrB proteins of *Streptomyces peucetius* in *Escherichia coli*: DrrA is an ATP binding protein. *J Bacteriol* 179: 569–575.
- Guilfoile PG, Hutchinson CR (1991) A bacterial analog of the *mdr* gene of mammalian tumor cells is present in *Streptomyces peucetius*, the producer of daunorubicin and doxorubicin. *Proc Natl Acad Sci U S A* 88: 8553–8557.
- Holm L, Rosenstrom P (2010) Dali server: Conservation mapping in 3D. *Nucleic Acids Res* 38: W545–9.
- Wilce JA, Vivian JP, Hastings AF, Otting G, Folmer RH, et al. (2001) Structure of the RTP-DNA complex and the mechanism of polar replication fork arrest. *Nat Struct Biol* 8: 206–210.
- Safo MK, Zhao Q, Ko TP, Musayev FN, Robinson H, et al. (2005) Crystal structures of the Blal repressor from *Staphylococcus aureus* and its complex with DNA: Insights into transcriptional regulation of the *bla* and *mec* operons. *J Bacteriol* 187: 1833–1844.
- Duggin IG, Andersen PA, Smith MT, Wilce JA, King GF, et al. (1999) Site-directed mutants of RTP of *Bacillus subtilis* and the mechanism of replication fork arrest. *J Mol Biol* 286: 1325–1335.
- Nguyen TKC, Tran NP, Cavin JF (2011) Genetic and biochemical analysis of PadR-padC promoter interactions during the phenolic acid stress response in *Bacillus subtilis* 168. *J Bacteriol* 193: 4180–4191.
- Licandro-Seraut H, Gury J, Tran NP, Barthelmebs L, Cavin JF (2008) Kinetics and intensity of the expression of genes involved in the stress response tightly induced by phenolic acids in *Lactobacillus plantarum*. *J Mol Microbiol Biotechnol* 14: 41–47.
- Gury J, Seraut H, Tran NP, Barthelmebs L, Weidmann S, et al. (2009) Inactivation of PadR, the repressor of the phenolic acid stress response, by molecular interaction with Usp1, a universal stress protein from *Lactobacillus plantarum*, in *Escherichia coli*. *Appl Environ Microbiol* 75: 5273–5283.
- Lim D, Poole K, Strynadka NC (2002) Crystal structure of the MexR repressor of the mexRAB-*oprM* multidrug efflux operon of *Pseudomonas aeruginosa*. *J Biol Chem* 277: 29253–29259.
- Cook WJ, Kar SR, Taylor KB, Hall LM (1998) Crystal structure of the cyanobacterial metallothionein repressor SmtB: A model for metalloregulatory proteins. *J Mol Biol* 275: 337–346.

Acknowledgments

We thank the staff of the ESRF (Grenoble) for providing facilities for diffraction measurements and for assistance.

Author Contributions

Conceived and designed the experiments: GF ATK OPK AMWHT. Performed the experiments: GF ATK TJP MB. Analyzed the data: GF ATK TJP MB AMWHT. Contributed reagents/materials/analysis tools: OPK AMWHT. Wrote the paper: GF ATK OPK AMWHT.